J|A|C|S COMMUNICATIONS

Published on Web 04/02/2009

Surface-Mediated Self-Coupling of Ethanol on Gold

Xiaoying Liu,[†] Bingjun Xu,[†] Jan Haubrich,[†] Robert J. Madix,[‡] and Cynthia M. Friend*[,†,‡]

Department of Chemistry and Chemical Biology and School of Engineering and Applied Sciences, Harvard University, 12 Oxford Street, Cambridge, Massachusetts 02138

Received February 2, 2009; E-mail: cfriend@seas.harvard.edu

Gold-based catalysis[1] has received tremendous interest since the discovery that gold nanoparticles supported on reducible metal oxide supports promote the catalytic oxidation of CO and alkenes at low temperature.[2,3] More recently, the use of gold catalysts to facilitate the aerobic oxidation of alcohols has become the center of attention,[4−10] affording the possibility of producing carbonyl derivatives through energy-efficient processes. In particular, ethanol is a potential future feedstock and its purification and conversion is of great importance for the chemical industry. Its derivative carbonyl compounds are important industrial chemicals and intermediate reagents that have wide applications in the food and perfume industries and other areas of synthetic chemistry.

The conversion of ethanol to acetaldehyde, acetic acid, and ethyl acetate catalyzed by Au nanoparticles in aqueous solution[9] and over O-covered Au[11,12] has been previously reported. Other alcohols, including primary[5,6,10,13] and secondary alcohols[5,10,13] as well as polyols such as glucose[14,15] are also oxidized by metallic Au. While a phenomenological model has been proposed for ethanol oxidation over supported Au catalysts,[9] a molecular-level understanding of the key intermediates and steps in the ethanol oxidation is necessary for optimizing reaction conditions and selectivity using microkinetic models.[16]

Fundamental studies of oxidation reactions on single-crystal Cu, Ag, and Au have provided the identity of reaction intermediates and elementary steps that are used for microkinetic models of (e.g.) methanol oxidation on Ag.[16] The established patterns of reactivity for adsorbed O, which acts as a Brønsted base on Cu and Ag, can be generalized to anticipate key features of Au chemistry.[12] Further, there are strong parallels between the oxidation of ethanol on oxidized Au(111) at low pressure and over Au supported on TiO_2 under high-pressure, aqueous phase conditions.[11]

Gold promotes O_2 dissociation much less efficiently than Ag or Cu[17,18] and adsorbed hydroxyl groups are less stable with respect to disproportionation to form water on Au.[19−21] Although there is still discussion regarding the possible efficacy of molecular oxygen species, such as superoxo or peroxide, in promoting oxidation reactions on Au, it has been clearly shown that O bound to Au efficiently drives oxidation reactions that parallel those observed on supported catalysts.[11] Indeed, the low dissociation probability for O_2, the reactive nature of adsorbed atomic oxygen, the instability of adsorbed OH, and the weak bonding of water result in low steady-state concentrations of surface species even at high pressure or in solution, rendering model studies under low pressure conditions relevant to higher pressure regimes.

In this work we establish the mechanism for the extremely facile transformation of ethanol to ethyl acetate, in competition with secondary oxidation to acetic acid, ketene ($H_2C{=}C{=}O$), and CO_2, over oxygen-covered Au(111). Esterification is very rapid, occurring below room temperature. We also address the possible underlying origins of the differences in our work, that was first reported as a preliminary study of ethanol oxidation on Au(111),[11] and subsequent work by Mullins et al.[22] that reported only intermediate oxidation to acetaldehyde.

Herein, we present a detailed study of ethanol oxidation on O-covered Au(111) in which we clearly demonstrate that the concentration of adsorbed oxygen plays a pivotal role in controlling reaction selectivity. The yield of the ester is a maximum at an initial O coverage of ∼0.2 ML. At these low oxygen coverages, our procedure for the deposition of O yields a surface comprising Au nanoparticles formed from O-induced release of Au from the surface. These particles mostly have diameters ≤ 2 nm[23] and with local 3-fold coordination of O.[24] At higher initial oxygen coverages, secondary oxidation to acetic acid, ketene, and CO_2 increases at the expense of ester formation. At these higher coverages, larger islands (>20 nm in diameter) of a 2-D "oxide" form.[23,24] Our results establish a trend for alcohol oxidation on Au and generalizes our recent findings for CH_3OH esterification, which is also favored at low oxygen coverage.[25] Furthermore, our results are consistent with liquid-phase catalytic oxidation of ethanol over supported Au nanoparticles.

Ozone was used to deposit atomic oxygen on Au(111), as described elsewhere.[26] Ethanol was dosed onto the oxygen-covered surface (denoted as O/Au(111)) at 180 K and heated at 5 $K \cdot s^{-1}$. Gaseous products were detected mass spectrometrically. Water does not accumulate on the surface during ethanol dosing since water desorbs rapidly at 180 K;[19−21] however, it does form due to oxidation reactions during heating.

For an initial O concentration of ∼0.05 ML, the predominant product of ethanol oxidation is ethyl acetate ($CH_3COOC_2H_5$, *m/z* 88 at 235 K) (Figure 1). There is no significant CO_2 or acetic acid evolution under these conditions, signifying nearly 100% selectivity for esterification. The only other products detected are ethanol and H_2O (Figure 1). There may be trace amounts of acetaldehyde (CH_3CHO, *m/z* 44 at 245 K); however, the overlap between the fragmentation patterns of ethanol and acetaldehyde preclude quantitative analysis. There are no fragment ions unique to acetaldehyde, and the production of ethanol in the same temperature regime rules out the use of either *m/z* 44 (parent ion of acetaldehyde) or *m/z* 29 (HCO^+) as a measure of CH_3CHO. The ester was identified by detection of the parent ion (*m/z* 88) and quantitative comparison of the fragmentation patterns of the products to those measured for an authentic sample condensed on clean Au(111) (Supporting InformationTable S1). The ethanol formed at 230 ± 5 K is reproducibly offset from the ester at 235 ± 5 K. Water is evolved in a broad peak at 225 ± 5 K, with a tail extending to 400 K. There is no residual oxygen, which shows that reaction of the adsorbed O with ethanol is facile (unreacted oxygen would evolve as O_2 in a peak at ∼550 K[26]). There is also no residual carbon detected.

[†] Department of Chemistry and Chemical Biology.
[‡] School of Engineering and Applied Sciences.

10.1021/ja900822r CCC: $40.75

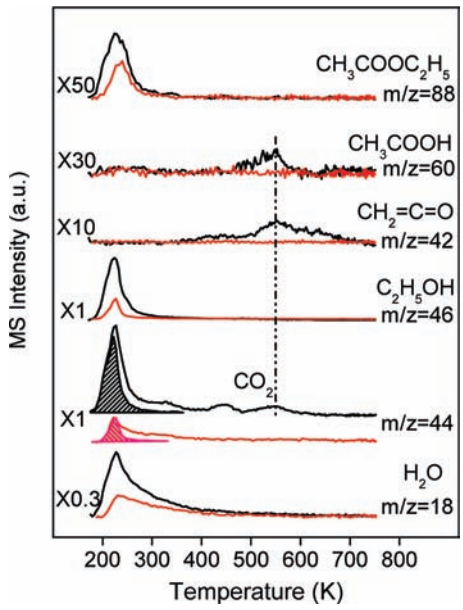

Figure 1. Temperature-programmed reaction of ethanol on O/Au(111) for two different initial oxygen coverages: 0.05 (red) and 0.2 ML (black). Ozone was dosed at a surface temperature of 200 K. The estimated contribution of fragmentation of ethanol to *m*/*z* 44 is shown by the shaded areas. The residual *m*/*z* 44 signal between 200 and 300 K is probably due to acetaldehyde evolution.

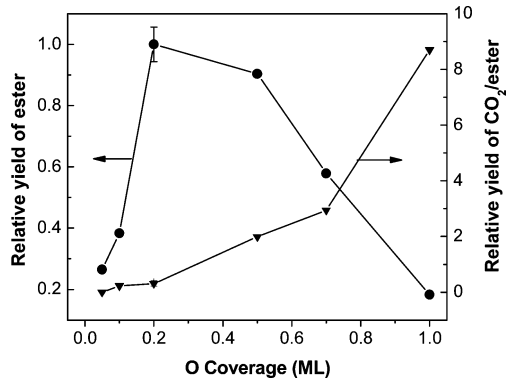

Figure 2. Dependence in the yield of the ester (ethyl acetate) and the ratio of CO_2:ester on the initial oxygen coverage in the oxidation of ethanol on Au(111). The initial surface concentration of atomic oxygen was varied by controlling the ozone flux. The relative yield of the ester was normalized with reference to the highest observed yield at 0.2 ML. The CO_2:ester ratio was determined from the integrated areas of *m*/*z* 44 and 88, correcting for the relative mass spectrometric sensitivities.

At higher O coverage (e.g., 0.2 ML), the yield of ethyl acetate increases and new products are formed, as is illustrated by comparing the temperature-programmed reaction data for oxygen coverages of ~0.05 and 0.2 ML (Figure 1). The yield of ethyl acetate is a maximum at ~0.2 ML of O, and several other products form. Acetic acid (CH_3COOH, *m*/*z* 60), ketene ($H_2C=C=O$, *m*/*z* 42), and CO_2 are all liberated concomitantly at 550 K, indicating that they originate in the same rate-limiting step at this O coverage. Above 0.2 ML of O the yield of the ester decreases as the yield of CO_2 increases (Figure 2); the yields of acetic acid and ketene increase when the O coverage is increased to 0.5 ML and level off until the saturation coverage is reached. The increased production of CO_2 along with acetic acid and ketene is attributed to secondary oxidation of transient acetaldehyde, based on studies of acetaldehyde oxidation on O/Au(111) (Supporting InformationFigure S1). Transient acetaldehyde also leads to ester formation, based on the fact

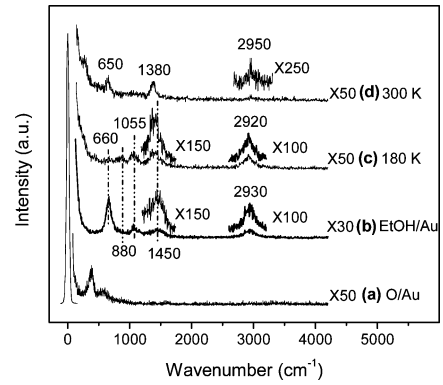

Figure 3. Vibrational spectra of the surfaces during the reaction of ethanol with O/Au(111). From bottom to top are (a) the as-prepared O/Au(111) with 0.2 ML of atomic oxygen deposited from ozone at 200 K (O/Au); (b) ethanol condensed on clean Au(111) at 180 K; (c) after exposure of ethanol to O/Au(111) at 180 K; and (d) after heating preparation c to 300 K. All spectra were collected at 180 K.

that coadsorption of acetaldehyde with equimolar amounts of ethanol increases the ethyl acetate yield by a factor of 2 (Supporting Information, Figure S2). At higher O coverages, there is probably a small amount of acetaldehyde evolution; however, the amount cannot be quantified because of the overlap with ethanol evolution. Overall, secondary oxidation increases at higher O coverage.

Additional mechanistic information is gained by identifying surface intermediates using vibrational (high resolution electron energy loss, HREEL) spectroscopy (Figure 3) (Supporting Information Table S2). As described above, the local bonding of oxygen on Au(111) depends on its coverage, based on the characteristic peaks in vibrational spectra. The peaks at 380 and 580 cm^{-1} are attributed to O in sites of local 3-fold coordination and to a surface oxide with two O atoms bound to a Au adatom, respectively,[24] for 0.2 ML of O deposited at 200 K (Figure 3a).

Ethanol reacts to form ethoxy by reaction of the alcoholic proton with adsorbed oxygen at 180 K, based on our vibrational data (Figure 3). The dissociation of the OH bond in ethanol is signified by the disappearance of the prominent γ(O−H) peak in ethanol at 660 cm^{-1} when adsorbed at 180 K on O-covered Au (Figure 3b,c). Other peaks characteristic of an intact ethoxy persist: 1055, 1450, and 2920 cm^{-1} (Figure 3c, Table S2). The two peaks associated with the initially adsorbed O also shift to lower frequency (280 and 440 cm^{-1}) and decrease in intensity. After annealing the surface to 300 K, a sharp feature appears at 1380 cm^{-1} that is a signature of an O−C−O backbone stretch (ν_{O-C-O}), typically assigned to carboxylate species.[27−29] The mode at 650 cm^{-1} is also typical of δ_{O-C-O} in carboxylates, for example, acetate.[29]

Ethoxy and acetate are indicated to be two important reaction intermediates in the oxidation of ethanol on Au(111). The formation of ethoxy is analogous to reaction patterns on Ag[30,31] and Cu[30,31] and to methoxy on O/Au(111)[25] and O/Au(110):[12] the alcoholic proton is transferred to adsorbed O in an acid−base reaction. Acetaldehyde is produced in an ensuing β-H elimination which is quite facile on O/Au(111). Ethyl acetate is formed from coupling of acetaldehyde and ethoxy,[11] substantiated by the fact that the yield of the ester increases when acetaldehyde is coadsorbed with ethoxy (Supporting Information Figure S2). Analogous esterification reactions were observed for methanol on O-covered Ag(110),[31] Au(110),[12] and Au(111).[25]

In competition, further oxidation of acetaldehyde leads to adsorbed acetate, which is detected spectroscopically. Under the conditions of our experiments, the adsorbed acetate disproportion-

ates to ketene and acetic acid with no net change in hydrogen content. Acetate also decomposes to CO_2 and H_2O. In aqueous media, in the presence of protons in solution, the acetate can convert to acetic acid, so no ketene would be formed, consistent with reported observations for supported catalysts.[8,9] Density functional theory studies are underway to interrogate the energetics of these reaction pathways and the roles of adsorbed O.

Our results provide the mechanistic framework below for catalytic oxidation of ethanol on supported catalysts and specifically show that the competing pathways involve two key intermediates: ethoxy and acetate.

$$2CH_3CH_2OH + O_{(a)} \rightarrow 2CH_3CH_2O_{(a)} + H_2O \quad (1)$$

$$CH_3CH_2O_{(a)} \rightarrow CH_3CHO_{(a)} + H_{(a)} \quad (2)$$

$$CH_3CHO_{(a)} + CH_3CH_2O_{(a)} \rightarrow CH_3COOCH_2CH_{3(g)} + H_{(a)} \quad (3)$$

$$CH_3CHO_{(a)} + O_{(a)} \rightarrow CH_3COO_{(a)} + H_{(a)} \quad (4)$$

$$2H_{(a)} + O_{(a)} \rightarrow H_2O_{(a)} \rightarrow H_2O_{(g)}\ (\text{fast}) \quad (5)$$

$$2CH_3COO_{(a)} \rightarrow CH_2{=}C{=}O_{(g)} + CH_3COOH_{(g)} + O_{(a)} \quad (6)$$

$$2CH_3COO_{(a)} + 7O_{(a)} \rightarrow 4CO_{2(g)} + 3H_2O_{(g)} \quad (7)$$

Our mechanism predicts that various reaction pathways—esterification, oxidative dehydrogenation to acetaldehyde, acetic acid production, and combustion—are linked. In particular, the yields of acetic acid and CO_2 are inextricably linked because both are derived from adsorbed acetate.

Under aqueous conditions, the selectivity for esterification increases with increasing ethanol concentration,[9] as expected from our mechanism. Oxygen is required for ethoxy formation and the ensuing steps; no measurable reaction of ethanol occurs on clean Au(111) (data not shown). Therefore, O must be deposited on supported Au under the higher pressure conditions. In solution, higher ethanol concentrations would increase the steady-state coverage of ethoxy, and therefore, decrease the O/ethoxy ratio, which would favor formation of the ester instead of acetic acid or CO_2. As ethoxy is converted to acetaldehyde two pathways compete: (1) esterification via direct attack of the aldehyde by ethoxy and (2) oxidation to acetate. The relative contributions of these pathways depend strongly on the oxygen coverage, with moderate oxygen coverages yielding both ester formation and secondary oxidation.

Given the strong parallels in ethanol oxidation over supported Au with Au crystals reported herein and in prior studies of O/Au(110)[12] and O/Au(111),[11] the qualitative difference in the product distribution reported by Mullins et al.[22] is surprising. Mullins et al. reported ~100% selectivity for acetaldehyde production on O/Au(111) (θ_o = 0.46 ML),[22] relying on *m*/*z* 29 for identification of acetaldehyde. Unfortunately, the *m*/*z* 29 fragment ion is common to ethanol and ethyl acetate, which we show are evolved in the same temperature regime. The *m*/*z* 29 may be due to a combination of ethanol and ethyl acetate fragmentation in both temperature-programmed reaction and steady-state measurements. However, two notable experimental differences between the studies exist: (1) a supersonic beam of oxygen atoms was used as the oxygen source by Mullins et al., whereas we employed O_3 decomposition; and (2) the surface temperature for ethanol exposure to the surface was 77 K in the Mullins' work compared to 180 K herein. While it is conceivable that the method of O deposition might lead to different surface structures, this is an unlikely explanation since prior work on O/Au(110) using an O atom source also showed that methanol couples to methyl formate.

In conclusion, the oxidation of ethanol on O/Au(111) strongly parallels the reaction patterns in solution-phase Au catalysis. The characteristics of Au—low steady-state concentrations of species, high selectivity because of the inertness of the metal toward bond activation, and the weak bonding of water and OH—make it a nearly unique case for bridging a wide range of reaction conditions. Our work shows the value of model studies, especially for Au-based chemistry, that provide a firm mechanistic basis for kinetic modeling of reaction selectivity.

Acknowledgment. We acknowledge the support of this work by the U.S. Department of Energy, Basic Energy Sciences, under Grant No. FG02-84-ER13289. R.J.M. gratefully acknowledges support from NSF CHE 9820703. The A. v. Humboldt Foundation also provided support for C.M.F. and J.H. (Feodor-Lynen program).

Supporting Information Available: Mass spectra fragmentation patterns for the identification of ethyl acetate, TPR spectra for the oxidation of acetaldehyde on Au(111), vibrational frequencies and band assignments for surface species in the oxidation of ethanol, and TPR spectra showing the dramatic increase of the yield of ethyl acetate with acetaldehyde coadsorbed with ethanol on O/Au(111). This material is available free of charge via the Internet at http://pubs.acs.org.

References

(1) Schwank, J. *Gold Bull.* **1983**, *4*, 103.
(2) Haruta, M.; Yamada, N.; Kobayashi, T.; Iijima, S. *J. Catal.* **1989**, *115*, 301.
(3) Min, B. K.; Friend, C. M. *Chem. Rev.* **2007**, *107*, 2709.
(4) Prati, L.; Rossi, M. *J. Catal.* **1998**, *176*, 552.
(5) Abad, A.; Concepcion, P.; Corma, A.; Garcia, H. *Angew. Chem., Int. Ed.* **2005**, *44*, 4066.
(6) Enache, D. I.; Knight, D. W.; Hutchings, G. J. *Catal. Lett.* **2005**, *103*, 43.
(7) Sheng, P. Y.; Bowmaker, G. A.; Idriss, H. *Appl. Catal., A* **2004**, *261*, 171.
(8) Christensen, C. H.; Jorgensen, B.; Rass-Hansen, J.; Egeblad, K.; Madsen, R.; Klitgaard, S. K.; Hansen, S. M.; Hansen, M. R.; Andersen, H. C.; Riisager, A. *Angew. Chem., Int. Ed.* **2006**, *45*, 4648.
(9) Jorgensen, B.; Christiansen, S. E.; Thomsen, M. L. D.; Christensen, C. H. *J. Catal.* **2007**, *251*, 332.
(10) Abad, A.; Almela, C.; Corma, A.; Garcia, H. *Tetrahedron* **2006**, *62*, 6666.
(11) Madix, R. J.; Friend, C. M.; Liu, X. Y. *J. Catal.* **2008**, *258*, 410.
(12) Outka, D. A.; Madix, R. J. *J. Am. Chem. Soc.* **1987**, *109*, 1708.
(13) Biella, S.; Rossi, M. *Chem. Commun.* **2003**, 378.
(14) Biella, S.; Prati, L.; Rossi, M. *J. Catal.* **2002**, *206*, 242.
(15) Prati, L.; Porta, F. *Appl. Catal., A* **2005**, *291*, 199.
(16) Andreasen, A.; Lynggaard, H.; Stegelmann, C.; Stoltze, P. *Surf. Sci.* **2003**, *544*, 5.
(17) Deng, X. Y.; Min, B. K.; Guloy, A.; Friend, C. M. *J. Am. Chem. Soc.* **2005**, *127*, 9267.
(18) McClure, S. M.; Kim, T. S.; Stiehl, J. D.; Tanaka, P. L.; Mullins, C. B. *J. Phys. Chem. B* **2004**, *108*, 17952.
(19) Wang, J.; Voss, M. R.; Busse, H.; Koel, B. E. *J. Phys. Chem. B* **1998**, *102*, 4693.
(20) Quiller, R. G.; Baker, T. A.; Deng, X. Y.; Colling, M. E.; Min, B. K.; Friend, C. M. *J. Chem. Phys.* **2008**, *129*, 064702.
(21) Ojifinni, R. A.; Froemming, N. S.; Gong, J. L.; Pan, M.; Kim, T. S.; White, J. M.; Henkelman, G.; Mullins, C. B. *J. Am. Chem. Soc.* **2008**, *130*, 6801.
(22) Gong, J.; Mullins, C. B. *J. Am. Chem. Soc.* **2008**, *130*, 16458.
(23) Min, B. K.; Alemozafar, A. R.; Pinnaduwage, D.; Deng, X. Y.; Friend, C. M. *J. Phys. Chem. B* **2006**, *110*, 19833.
(24) Baker, T. A.; Xu, B. J.; Liu, X. Y.; Kaxiras, E.; Friend, C. M. Unpublished work.
(25) Xu, B. J.; Liu, X. Y.; Haubrich, J.; Madix, R. J.; Friend, C. M. Angew. Chem., Int. Ed. DOI: 10.1002/anie.200805404.
(26) Saliba, N.; Parker, D. H.; Koel, B. E. *Surf. Sci.* **1998**, *410*, 270.
(27) Sexton, B. A.; Madix, R. J. *Surf. Sci.* **1981**, *105*, 177.
(28) Sim, W. S.; Gardner, P.; King, D. A. *J. Phys. Chem.* **1995**, *99*, 16002.
(29) Haley, R. D.; Tikhov, M. S.; Lambert, R. M. *Catal. Lett.* **2001**, *76*, 125.
(30) Wachs, I. E.; Madix, R. J. *Appl. Surf. Sci.* **1978**, *1*, 303.
(31) Liu, X. Y.; Madix, R. J.; Friend, C. M. *Chem. Soc. Rev.* **2008**, *37*, 2243.

JA900822R